Orientable pore-size-distribution of ZnO nanostructures and their superior photocatalytic activity

Xiaowei Duan, Guozhong Wang,* Hongqiang Wang, Yongqiang Wang, Chen Shen and Weiping Cai

Received 29th October 2009, Accepted 11th March 2010
DOI: 10.1039/b922679f

Rod-like ZnO micro-nanostructures have been synthesized by a solvothermal-assisted heat treatment method. The micro-nanostructures consist of polycrystalline nanoparticles with a hexagonal wurtzite structure. The diameter and length of the nanorods are about 90–150 nm and 0.6–3 μm, respectively. Nitrogen sorption isotherm analysis reveals a bi-pore-size-distribution feature of ZnO micro-nanostructures and the origin of this peculiar pore-size distribution may be ascribed to the polar feature of ZnO crystals. Importantly, these micro-nanostructures have superior photocatalytic activity and high durability in the degradation of organic dyes.

1. Introduction

Environmental problems, such as organic pollutants and toxic chemicals, provide the impetus for fundamental and applied research in the environmental area. Semiconductor absorbents and photocatalysts offer the potential for elimination of toxic chemicals through their efficiency and broad applicability.[1] ZnO nanoparticles can be utilized for the degradation of organic pollutants in nearly neutral solution, because of their high specific surface area which will supply more chances for the encounter of the produced electron-hole pair with the dye molecules,[2] and due to sterilization of bacteria and viruses by the hydrogen peroxide generated from photocatalysis.[3–6] However, there are two disadvantageous points that affect the durability of ZnO photocatalyst in the practical application, one is the unavoidable aggregation of the nanoparticles during aging and the other is the difficulty in reclaiming the nanoparticles because of their small size. One possible solution to this problem is to create a micro-nanostructrue, which not only maintains a high surface-to-volume with strong activity but also prevents further aggregation and also facilitates recovery of the nanoparticles due to the larger particle size. Also the durability of ZnO nanostructure based photocatalyst was still a difficult technological issue to solve.[7,8]

Therefore, creating a novel ZnO nanoarchitecture that is stable against aggregation and possesses a high porosity and large specific surface area, which are needed for environmental remediation applications, is desirable. In our previous work, we synthesized corn-like ZnO nanorods which consist of nanoparticles, and here experimental results reveal that the nanoarchitechtures are made up of bi-pore-size-distribution micro-nanostructures. Importantly, such ZnO structures show superior photocatalytic activity and durability, providing an alternative way to improve the photocatalytic durability of ZnO nanoparticles.

Key Laboratory of Materials Physics, Anhui Key Laboratory of Nanomaterials and Nanotechnology, Institute of Solid State Physics, Chinese Academy of Sciences, Hefei, 230031, P.R. China. E-mail: gzhwang@issp.ac.cn

2. Experiment

Synthesis

Preparation of bi-pore-size-distribution ZnO micro-nanostructures. Zinc acetate dihydrate ($Zn(CH_3COO)_2 \cdot 2H_2O$), >99%, Shanghai Dongyi Chemical Reagent Co. Ltd, AR) and oxalic acid ($C_2H_2O_4 \cdot 2H_2O$, >99.5%, Tianjin Daishi Chemical Reagent Co. Ltd, AR) was used without purification. The preparation of as-prepared ZnO micro-nanostructure was similar to that reported in the literature.[9] Zinc acetate dihydrate (25 mmol) and oxalic acid dihydrate (25 mmol) were added to 40 mL alcohol (C_2H_5OH, >99.7%, Shanghai Zhengxing Chemical Plant, AR) under stirring until the mixture became the gel. The above solution was mixed homogeneously and transferred into a Teflon lined stainless-steel autoclave (70 mL) and heated to a temperature of 80 °C for 5 h. After cooling to room temperature, the precipitate was washed repeatedly with deionized water, and then dried at 60 °C for 1 h. After the obtained white powder was annealed at 450 °C for 2 h in a muffle furnace, the bi-pore-size-distributed ZnO micro-nanostructure was finally obtained.

Preparation of ZnO nanorods. 80 mL of 0.1 M $ZnCl_2$ (>98%, Shanghai Guoyao Chemical Reagent Co. Ltd, AR) solution was first prepared, and then 4 mL ammonia (25–28%, Shanghai Zhongshi Chemical Company, AR) was dropped slowly (about 0.6–0.8 mL min^{-1}) into the solution under stirring for 10 min. The solution was then transferred into a 170 mL Teflon autoclave. A silicon wafer suspended horizontally about 5 mm below the solution surface was used to collect the products. The autoclave was put in an oven at 95 °C for 90 min. Finally the autoclave was cooled down naturally to room temperature, and the substrate was rinsed with deionized water several times to remove any residual salts or amine complexes in the final product and dried naturally before further characterization.

Characterization

The phase of the product was identified by X-ray diffraction analysis (XRD, Philips X'pert PRO) using Ni-filtered monochromatic CuKα radiation at 40 keV and 40 mA. The

morphology and size of the products was characterized by field emission scanning electron microscope (FESEM, Sirion 200 FEG) using an accelerating voltage of 5.00 kV, and transmission electron microscopy (TEM, JEOL-2010, 200 kV) with an energy dispersive X-ray spectrometer (EDX). The powders were ultrasonically-dispersed in ethanol. The suspension was then dropped onto the SEM stub and holey-carbon grid for SEM and TEM examination respectively. The surface area of the samples was determined by nitrogen adsorption (Micrometrics ASAP 2020) using the five-point Brunauer–Emmet–Teller (BET) isotherm.

Photocatalytic activity measurement

The reaction suspension was prepared by adding 20 mg as-prepared ZnO micro-nanostructure into 80 mL of methyl orange (MO, 10^{-5} M) solution. The suspension was irradiated using a high-pressure Hg lamp (125 W, 8 cm away from the suspension) under continuous stirring at room temperature (an electric fan was used to avoid temperature increase of the reaction solutions during UV light irradiation). Before irradiation, the aqueous solution was stirred in the dark for 30 mins to reach the adsorption equilibrium of MO with the catalyst. Analytical samples for absorption measurement were taken out from the reaction suspension at different time intervals, and 4 mL solution was taken every time and centrifuged at 7000 rpm for 2 mins to remove the as-prepared ZnO micro-nanostructure. A spectrophotometer (CARY-5E) was used to record the UV-vis absorption spectra of the centrifuged solutions. Further comparative experiments including 20 mg Degussa P25 titania powders, 20 mg ZnO nanorods, 20 mg commercial ZnO microparticles were also carried out to investigate the photocatalytic activity. The durability of the photocatalytic activity of the as-prepared ZnO micro-nanostructure was also studied by reuse of the catalysts under the UV light irradiation, which was performed at the same ratio of the as-prepared ZnO micro-nanostructure to MO. After the first cycle, all of the solutions, including the taken-out samples, were recovered to centrifuge, wash and distill. The obtained powders were reused in the second cycle. The processes of the second and third cycles were as above.

The photocatalytic activity of the as-prepared ZnO micro-nanostructure was also tested in photodegrading organic dyes of methylene blue (MB, 10^{-5} M). The experiment of photodegrading MB was performed under the same conditions as the first cycle of photodegrading MO.

3. Results and discussion

Characterization of bi-pore-size-distribution ZnO micro-nanostructures

An X-ray diffraction pattern of the as-prepared products is shown in Fig. 1a, in which the diffraction of standard hexagonal (wurtzite) ZnO powders is also included (JCPDS 36-1451). All the diffraction peaks can be indexed to the wurtzite ZnO. FESEM was employed to investigate the morphology of the as-prepared sample (Fig.1b). A high magnification image (insert of Fig. 1b) further reveals that the rod-like structure is composed of small ZnO nanoparticles (average diameter is about 20 nm). One can see that the diameter of the rods mainly varies from 90 to 150 nm, and the length ranges from 0.6 to 3 μm. Further structural

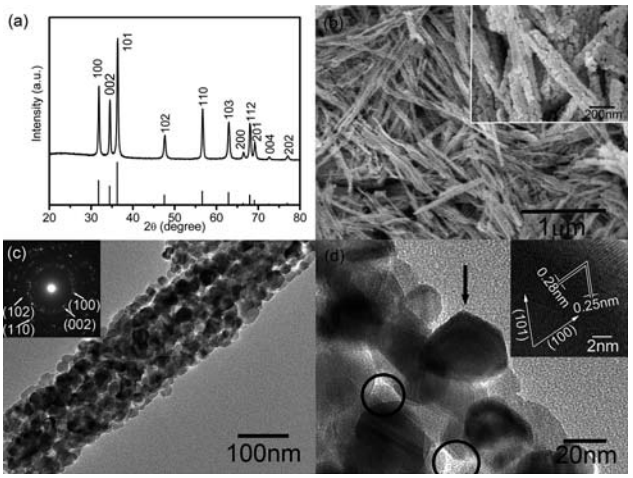

Fig. 1 (a) XRD patterns of the as-prepared products obtained from the solvothermal method and heated at 450 °C for 2 h and the standard ZnO (JCPDS no. 36-1451); (b) Low-magnification SEM image of as-prepared ZnO micro-nanostructures (the inset shows the high-magnification view of typical ZnO structures); (c) TEM image of one as-prepared ZnO micro-nanostructure (the inset shows the corresponding SAED pattern); (d) High magnification TEM image of a section of the as-prepared ZnO micro-nanostructures (the inset presents a HRTEM image taken from the particle indicated by the arrow).

characterization of the as-prepared ZnO micro-nanostructure was performed by TEM. Obviously, there are many nanoholes in the nanorods (shown in Fig. 1c and 1d), which range from several to tens of nanometres marked clearly in Fig. 1d. Careful examination reveals that the nanoparticles arrange more closely along the axis direction than the radial direction, which makes the different sizes of the nanoholes between the axis and the radial. The inset of Fig. 1c presents the selected area electron diffraction (SAED) pattern, which indicates that the as-prepared ZnO micro-nanostructures have a polycrystalline structure. The inset of Fig. 1d shows a high-resolution transmission electron microscopy (HRTEM) image of one particle of the as-prepared ZnO micro-nanostructure (indicated by the arrow). The interplanar spacing is about 0.28 and 0.25 nm corresponding to the (100) and (101) plane of the hexagonal structure of ZnO, respectively.

To give further insight into the porous structure and pore-size distribution of the as-prepared products, the nitrogen sorption isotherms were measured by Accelerated Surface Area and Porosimetry (ASAP) to examine the characteristics of the pores. As shown in Fig. 2, the nitrogen adsorption-desorption isotherm belongs to type IV, revealing the existence of abundant mesoporous structures in the architectures. From the corresponding pore size distribution curves (inset in Fig. 2), we find that the pore size distribution is not uniform, and the pore sizes are mainly distributed around the sizes of 3 and 30 nm, which is in agreement with the results of the TEM analysis (see Fig. 1c and 1d). Note that the peak around 3 nm is derived from the close arrangement of the nanoparticles along the axis, and the larger size of the pores of 30 nm is mainly attributed to the loose arrangement of nanoparticles along the radial direction. The specific surface area of the as-synthesized ZnO is evaluated to be approximately 20.87 m^2 g^{-1} by BET equation, which is larger

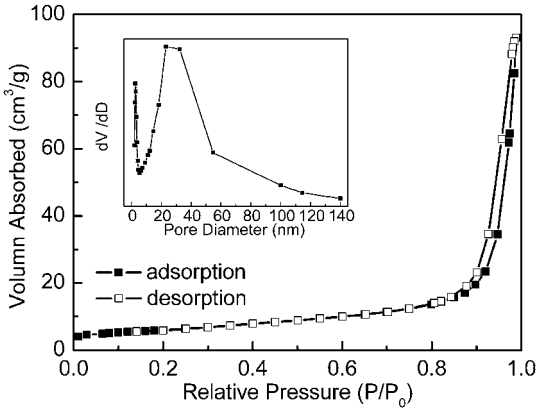

Fig. 2 Full nitrogen sorption isotherms of the as-prepared sample (the inset shows pore size distribution).

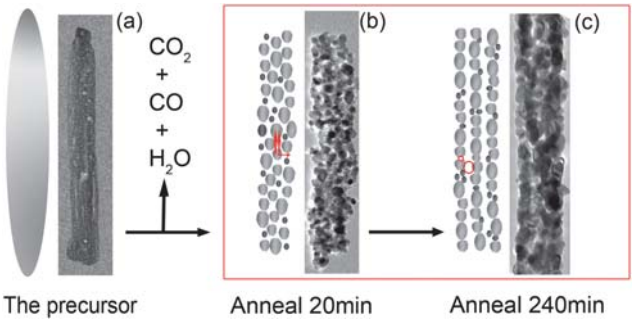

Fig. 3 Schematic illustrations of the formation mechanism of the bi-pore-size-distributed ZnO micro-nanostructures: (a) formation of a precursor $ZnC_2O_4 \cdot 2H_2O$ nanorod, (b) formation of ZnO nanorods with disordered nanoparticles, (c) realignment of the nanoparticles along the axis in nanorods.

than that of commercial ZnO powders (*ca.* 4–5 $m^2\ g^{-1}$). Obviously, this hierarchically structured ZnO with high specific surface area, relative to ZnO nanoparticles, will effectively prevent aggregation, and may exhibit potential application in catalysis and sensing.

Formation of the bi-pore-size-distribution ZnO micro-nanostructures

A growth mechanism of the bi-pore-size-distribution ZnO micro-nanostructures can be proposed as follows. From the crystallography, ZnO can be described as a number of alternating planes composed of tetrahedrally coordinated O^{2-} and Zn^{2+} ions, stacked alternately along the c axis.[10] Generally, the positively Zn^{2+} terminated (001) and negatively O^{2-} terminated (00 $\bar{1}$) polar surfaces have high surface energies, and the growth and aggregation of the crystal will be preferentially along the c axis. In the present study, the precursor of $ZnC_2O_4 \cdot 2H_2O$ was very important and served as the template in the formation of the as-prepared ZnO micro-nanostructures. The formation of the precursor is described by the following reactions:[9]

$$Zn(CH_3COO)_2 \cdot 2H_2O + H_2C_2O_4 \cdot 2H_2O \rightarrow ZnC_2O_4 \cdot 2H_2O + 2CH_3COOH + 2H_2O \quad (1)$$

$$CH_3COOH + C_2H_5OH \rightarrow CH_3COOC_2H_5 + H_2O \quad (2)$$

The source materials of $Zn(CH_3COO)_2 \cdot 2H_2O$, $H_2C_2O_4 \cdot 2H_2O$ and C_2H_5OH were used in the reactions as described by eqn (1) and eqn (2). Eqn (2) accelerates eqn (1) forward and thus helps the formation of $ZnC_2O_4 \cdot 2H_2O$. The morphology of $ZnC_2O_4 \cdot 2H_2O$ was confirmed by the SEM investigation, which showed rod-like structures (shown in the inset of Fig. 3a). The formation of the bi-pore-size-distribution ZnO micro-nanostructures from the rod-like precursor of $ZnC_2O_4 \cdot 2H_2O$ can be divided into two separate steps, *i.e.*, the decomposition of the precursor, $ZnC_2O_4 \cdot 2H_2O$, and the realignment of ZnO nanoparticles. Fig. 3 demonstrates the formation mechanism, and shows the corresponding TEM images of the precursor in the different stages. First, the precursor, $ZnC_2O_4 \cdot 2H_2O$, evolves to ZnO micro-nanostructures according to the following reaction:[9]

$$ZnC_2O_4 \cdot 2H_2O \rightarrow ZnO + CO + CO_2 + H_2O \quad (3)$$

Initially, the decomposition of $ZnC_2O_4 \cdot 2H_2O$ leads to the release of gases CO, CO_2 and H_2O *via* heat-treatment, which results in the holes among the disordered nanoparticles in ZnO nanorods (shown in Fig. 3b). Fig. 3b shows a rod-like ZnO nanostructure composed of disordered nanoparticles; the double red arrow indicates the axis direction and the single red arrow indicates the radial direction. As the reaction time lengthens, the nanopore sizes along the axis is are smaller than those along the radial, which causes bi-pore-size-distributed structure (shown in Fig. 3c). We propose that oriented attachment of the ZnO nanoparticles occurs along the c axis,[11–14] and the highest surface energy of the c plane advances the aggregation of nanoparticles along the c-axis,[10] which results in the closer arrangement of nanoparticles along the axis than along the radial. Therefore, the formation of bi-pore-size-distribution ZnO micro-nanostructures is mainly determined by the internal structure of the precursor crystal and the oriented attachment.

Photocatalytic activity

In order to investigate the photocatalytic characteristics of the as-prepared ZnO micro-nanostructures, methyl orange (MO), a typical anionic organic pollutant in the textile industry, has been chosen as the photocatalytic degration dye. The top of Fig. 4 shows a series of color changes corresponding to the sequential change of the absorption measurements of MO aqueous solution with the as-prepared ZnO micro-nanostructure powders after exposure to UV light for different durations. It is clear that the intense orange color of the starting solution gradually disappears with increasing exposure time to the UV light.

Further comparative experiments were carried out to investigate the photocatalytic activity of the as-prepared ZnO micro-nanostructures, commercial ZnO microparticles (size 2–3 μm), ZnO nanorods (diameter 200 nm), Degussa P25 titania powders (size 20 nm). It could be observed that the absorption peak of MO molecules still exists after 60 mins exposure time for ZnO microparticles and nanorods, while for the Degussa P25 titania powders, the absorption peak nearly disappears after about 30

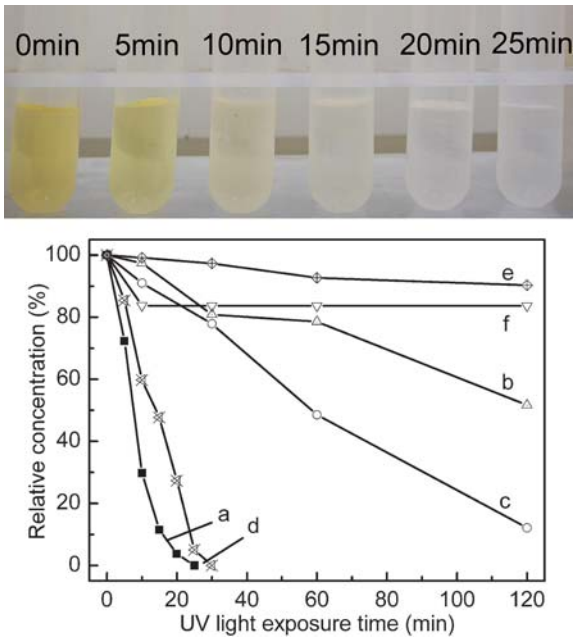

Fig. 4 The top photograph shows time-dependent colour change of MO solution in the presence of as-prepared ZnO micro-nanostructures; The bottom is MO normalization concentration (the optical absorbance measurements at 464 nm) in the solution (80 mL) with different catalysts (20 mg) *versus* the exposure time to UV light. Starting MO concentration C_0: 1.0×10^{-5} M. As-prepared ZnO micro-nanostructure powders (curve a), commercial ZnO microparticles powders (curve b), ZnO nanorods powders (curve c), Degussa P25 titania powders (curve d), commercial rutile TiO_2 powders (curve e) and 20 mg of as-prepared ZnO micro-nanostructures without UV light irradiation (curve f).

mins of exposure time. The comparative results shown in the bottom of Fig. 4 demonstrate that the degradation rate of MO for the as-prepared ZnO micro-nanostructure (curve a) is much higher than that of commercial ZnO microparticles powders (curve b), ZnO nanorods powders (curve c) and commercial rutile TiO_2 powders (curve e). After 60 mins irradiation, 78.54% and 48.56% MO still exist for the commercial ZnO microparticles and ZnO nanorods powders respectively, and 92.73% remained for the commercial rutile TiO_2 powders. The whole degradation speed of the Degussa P25 titania powders is similar to that of the as-prepared ZnO micro-nanostructure (see curve a and d), but the Degussa P25 titania powders is uncompleted in 25 mins, with 5% remaining as shown in Fig. 4b.

Although the specific surface area of the as-prepared ZnO micro-nanostructures (20.87 m^2g^{-1}) is smaller than that of the Degussa P25 titania powders (50 m^2g^{-1}), the MO degradation rate of the former is faster than that of the latter. Comparatively, unwanted aggregation during the reaction usually leads to a significant decrease in the active surface area and thus the photocatalytic performance of Degussa P25 nanopowders.[1] On the other hand, the photocatalytic efficiency is surface-dependent to some extent, and the organic dyes could be degraded only if they adsorb on the surface of the catalyst.[15]

It should be noted that it took less than about 10 mins to reach the maximum adsorption capacity on the as-prepared ZnO micro-nanostructure with about 16% decrease of MO concentration (curve f). This fast adsorption rate and nearly 16% decrease of MO concentration are considered to be related to the peculiar porous nanostructure. Nevertheless, when the MO reaches 100% degradation, the room-temperature photodegradation of the as-prepared ZnO micro-nanostructure dominates the decrease of MO concentration. The origin of the higher photocatalytic activity of the as-prepared ZnO micro-nanostructure is mainly ascribed to the high specific surface area of the polycrystalline structure (shown in Fig. 1c). However, this point alone cannot fully explain the fast degradation. For the porous ZnO micro-nanostructure in the present study, there are two unique advantages in the photocatalysis, which might be helpful to understand the fast photocatalysis performance: (i) the nanoholes in ZnO nanorods provide ideal channels for easy and fast diffusion of the dye molecules to contact the different interplanar surfaces of the nanoparticles, which greatly increases the chances and velocities of the encounter of the produced electron-hole pair with the dye molecules and thus enhances the photocatalytic activity; (ii) the nanoholes with bi-pore-size-distribution in ZnO nanorods, the bigger pore-size nanoholes along the radial are transparent for UV light, which greatly increases the utilizing efficiency of UV light.[8]

The durability of the photocatalytic activity of the as-prepared ZnO micro-nanostructure and the Degussa P25 titania was also studied by reuse of the catalysts in fresh MO under UV light irradiation, which was performed at the same conditions of the as-prepared ZnO micro-nanostructure and MO. Fig. 5 shows the photodegradation results for three cycles using the as-prepared ZnO micro/nanostructure and Degussa P25 titania (25 mins irradiation for each cycle). The as-prepared ZnO micro-nanostructure exhibits the same superior durability as Degussa P25 titania and there is no significant change in the activity even after the third cycle. Compared with porous ZnO nanotubes decreasing 7.5% after five cycles[8] and ZnO hierarchical structures decreasing 5% after three cycles,[7] the durability of the photocatalytic activity of the as-prepared ZnO micro-nanostructure is very excellent, it can be seen that the degradation rate is not decreasing on the whole after three cycles. This excellent durability of the photocatalytic activity of the as-prepared ZnO micro-nanostructures is probably ascribed to the special bi-pore-size-distributed structure. The dense arrangement along c axis maintains the stability of the structure to the maximum extent,

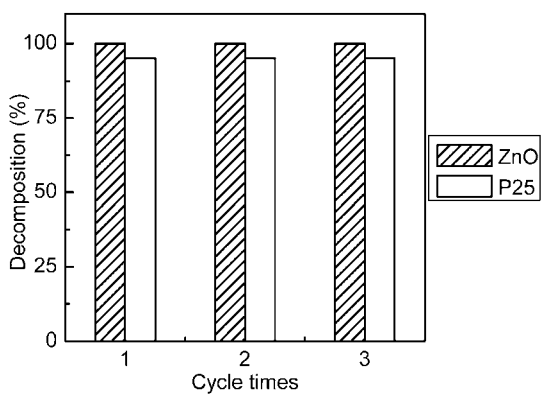

Fig. 5 Comparison of the durability of the as-prepared ZnO micro-nanostructures and Degussa P25 titania (P25) under UV light for the three cycles.

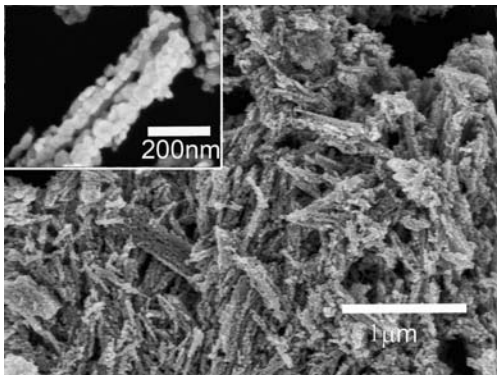

Fig. 6 SEM image of the as-prepared products after the first cycle.

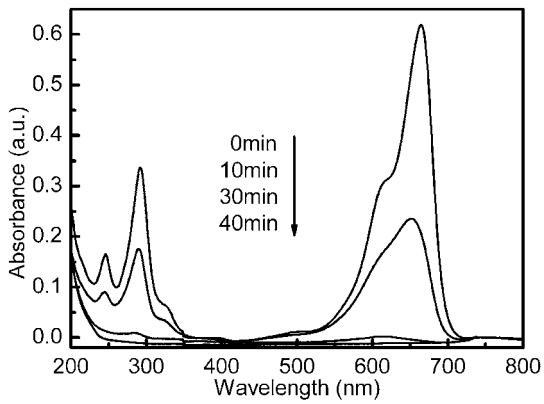

Fig. 7 Time-dependent optical absorbance spectra of the MB solution with the as-prepared ZnO micro-nanostructure.

and the loose nanoholes provide ideal channels for the dye molecules and UV light. One can see that after the first cycle, the morphology of the as-prepared ZnO micro-nanostructures scarcely changes (Fig. 6). In the photocatalytic process, aggregation and photocorrosion of the as-prepared ZnO micro-nanostructures was scarcely found.

In addition, the photocatalytic activity of the as-prepared ZnO micro-nanostructures was also tested in photodegrading the organic dye methylene blue (MB, 10^{-5} M), a cationic organic dye, Fig. 7. Under the same experimental conditions, the as-prepared ZnO micro-nanostructure also has excellent photocatalytic activity for the degradation of cationic organic pollutants.

4. Conclusions

In summary, orientable pore-size-distribution ZnO micro-nanostructures have been successfully prepared by a two-step method, involving a low temperature solvothermal and heat treatment process. The formation mechanism of the porous ZnO micro-nanostructures is mainly governed by the oriented attachment more preferential along the c axis than along the radial directions. Superior photocatalytic activity of the as-prepared ZnO micro-nanostructure in the degradation of MO compared to commercial ZnO microparticles powders, ZnO nanorods powders, Degussa P25 titania powders and commercial rutile TiO_2 powders has been demonstrated. The origin of the higher photocatalytic activity of the as-prepared ZnO micro-nanostructure is mainly ascribed to the high specific surface area of the polycrystalline structure. In addition, the nanoholes in ZnO nanorods provide ideal channels for easy and fast diffusion of the dye molecules to contact the different interplanar surfaces of the nanoparticles, and also greatly increases the efficiency of UV light. Moreover, the as-prepared ZnO micro-nanostructure has higher durability to photodegradation than other ZnO nanostructures, the same as Degussa P25 titania powders. The as-prepared ZnO micro-nanostructure is expected to find potential applications in environmental remediation and toxic chemicals treatment.

Acknowledgements

This work is supported by the National Basic Research Program of China (Grant No. 2007CB936604), the Natural Science Foundation of China (Grant No. 50302010), the Scientific Research Foundation for the Returned Overseas Chinese Scholars, State Education Ministry and Special Foundation of President of Hefei Institutes of Physical Science, the Chinese Academy of Sciences, and the Hundred Talent Program of the Chinese Academy of Sciences.

References

1 J. S. Hu, L. L. Ren, Y. G. Guo, H. P. Liang, A. M. Cao, L. J. Wan and C. L. Bai, *Angew. Chem., Int. Ed.*, 2005, **44**, 1269.
2 H. B. Lu, H. Li, L. Liao, Y. Tian, M. Shuai, J. C. Li, M. F. Hu, Q. Fu and B. P. Zhu, *Nanotechnology*, 2008, **19**, 045605.
3 A. J. Hoffman, E. R. Carraway and M. R. Hoffmann, *Environ. Sci. Technol.*, 1994, **28**, 776.
4 E. R. Carraway, A. J. Hoffman and M. R. Hoffmann, *Environ. Sci. Technol.*, 1994, **28**, 786.
5 K. Sato, M. Aoki and R. Noyori, *Science*, 1998, **281**, 1646.
6 C. H. Ye, Y. Bando, G. Shen and Z. D. Golberg, *J. Phys. Chem. B*, 2006, **110**, 15146.
7 F. Lu, W. P. Cai and Y. G. Zhang, *Adv. Funct. Mater.*, 2008, **18**, 1047.
8 H. Q. Wang, G. H. Li, L. C. Jia, G. Z. Wang and C. J. Tang, *J. Phys. Chem. C*, 2008, **112**, 11738.
9 L. Yang, G. Z. Wang, C. J. Tang, H. Q. Wang and L. D. Zhang, *Chem. Phys. Lett.*, 2005, **409**, 337.
10 L. Vayssieres, *Adv. Mater.*, 2003, **15**, 464.
11 Claudia Pacholski, Andreas Kornowski and Horst Weller, *Angew. Chem., Int. Ed.*, 2002, **41**, 1188.
12 J. F. Banfield, S. A. Welch, H. Zhang, T. T. Ebert and R. L. Penn, *Science*, 2000, **289**, 751.
13 R. L. Penn and J. F. Banfield, *Science*, 1998, **281**, 969.
14 R. L. Penn and J. F. Banfield, *Geochim. Cosmochim. Acta*, 1999, **63**, 1549.
15 E. S. Jang, J.-H. Won, S.-J. Hwang and J.-H. Choy, *Adv. Mater.*, 2006, **18**, 3309.